Three-dimensional neutron-depolarization analysis of the magnetic flux distribution in $YBa_2Cu_3O_{7-\delta}$

W. Roest and M. Th. Rekveldt
Interfaculty Reactor Institute, Delft University of Technology, 2629 JB Delft, The Netherlands
(Received 15 March 1993)

In this paper, a three-dimensional neutron-depolarization analysis of the vortex distribution in sintered $YBa_2Cu_3O_{7-\delta}$ is described. In the experiment, the sample is zero-field cooled after which, at 4.2 K, a magnetic-field pulse with a width of 500 μs and a peak value of 0.7 T is applied. After this pulse the remanent field in the sample is of the order of 0.01 T and shows no measurable time decay within 24 h. By heating the sample and measuring the depolarization matrix with the three-dimensional method, the remanent field and the average flux distribution trapped in the ceramic superconductor are determined from one and the same measurement. The results show a distribution of flux that is not homogeneous, and flux lines that are bundled and bent at low temperatures together with a nonlinear decay of remanent magnetization as a function of temperature. At temperatures close to T_c, the distribution becomes homogeneous and the temperature dependence linear.

I. INTRODUCTION

Since the discovery of superconductivity, many studies have been performed on the distribution of flux vortices in type-II superconductors. Most of the methods used are surface or thin-film methods, rather than bulk studies. However, several neutron-scattering techniques are very suitable for bulk investigations. Very recently a small-angle neutron-scattering (SANS) experiment on a high-T_c single crystal was performed,[1] showing evidence for a square and a hexagonal flux lattice. For these short-range correlations, SANS is a very suitable method, but for larger-scale correlations of flux or flux distributions, neutron depolarization is more appropriate.

Neutron depolarization has successfully been used to investigate conventional type-II superconductors,[2] but only a limited number of experimental results on the high-T_c superconductors are published.[3–6] Most of these published results are discussed and interpreted in a qualitative way.

In the neutron-depolarization experiments presented in this paper, the analysis is done in three dimensions, which enables us to follow the precession and the shortening of the polarization vector of the neutron beam due to the remanent magnetization inside the high-T_c superconductor $YBa_2Cu_3O_{7-\delta}$. This analysis is called three-dimensional neutron depolarization (3DND).

3DND, described in 1973,[7] appeared to be an easy and accurate method of determining simultaneously the correlation length of local magnetic structures and the magnitude and direction of an average magnetization in bulk samples, statically[8,9] as well as dynamically.[10,11] The measurable range of the correlation length starts at 10 nm and goes up to millimeters.

Here, only a brief description of the 3DND setup and theory will be given. An extended description is given in Refs. 8 and 9. The neutron source used in the experiments is the 2-MW swimming pool type reactor (HOR) at the Interfaculty Reactor Institute (IRI) in Delft, the Netherlands. The neutron beam coming from this source is spin polarized by a magnetized Cu_2MnAl crystal and can be offered at a magnetically shielded sample position with a polarization direction in either the x, y, or z direction. The directions are defined as the beam, horizontal, and vertical directions, respectively. After transmission through a sample with a certain magnetic structure, the polarization of the beam can be analyzed in the same three directions. The quality of the polarizing and analyzing systems are described by a matrix $\underline{P}$ and $\underline{Q}$, respectively.[12] When all possible combinations of polarizing and analyzing directions are taken, a 3×3 matrix $\underline{D}_m$ is measured. The elements of this matrix are given by

$$D_{m,ij} = 1 - \frac{I_{ij}}{I_s}, \qquad i,j = x,y,z. \tag{1}$$

Here I_{ij} is the measured intensity and I_s the intensity of the fully depolarized beam, called the "shim intensity."

When a polarized neutron beam is passing through a time-dependent magnetic induction $\mathbf{B}(t)$, the change of the polarization vector $\mathbf{p}$ in time can be written as

$$\frac{d\mathbf{p}(t)}{dt} = \gamma\,[\mathbf{p}(t) \times \mathbf{B}(t)], \tag{2}$$

with γ the gyromagnetic ration of the neutron ($\gamma = 1.83 \times 10^8\ \mathrm{s^{-1}\,T^{-1}}$). When the neutron beam passes through a sample containing a certain magnetic structure, Eq. (2) can be solved, leading to the following polarization vector $\mathbf{p}_f$ at the analyzing position:

$$\mathbf{p}_f = \underline{D}_t \mathbf{p}_0, \tag{3}$$

where the matrix $\underline{D}_t$ is equivalent to the measured ma-

trix. In $\underline{D}_t$, two effects are combined, the Larmor precession around the mean magnetic induction and the depolarization caused by local fluctuations in this average induction over the beam cross section.

For the purpose of the calculation, the sample is divided into N small parts, each representative for the whole sample. The precession in each part is small and can be separated from the depolarization. Both the rotation of the polarization vector and the depolarization can be described with a matrix. The rotation matrix will be denoted by $\underline{R}$, with $\underline{R}$ given by

$$\underline{R} = \underline{U} + \underline{S}\sin\phi + \underline{S}^2(1-\cos\phi); \tag{4}$$

where

$$\underline{S} = \begin{pmatrix} 0 & -n_z & -n_y \\ n_z & 0 & -n_x \\ n_y & n_x & 0 \end{pmatrix}.$$

Here $\phi = c\lambda L\langle B\rangle$ is the rotation angle of the polarization vector around the average induction $\langle B\rangle$ where λ is the neutron wavelength, $c \equiv \frac{\gamma m}{h}$ with m the neutron mass, h Planck's constant, and $L = t/N$ the transmission length of one sample part. The quantity t is the total transmission length and n_i $(i = x, y, z)$ are the projections of the unit vector of the magnetic induction on the x, y, and z axes, respectively. $\underline{U}$ is the unit matrix.

In order to be able to make a description of the depolarization, one must realize what is really measured in a 3DND experiment. In Ref. 9, a clear description is given of the derivation of the elements of the depolarization matrix. To derive an expression for these elements, one needs to calculate the averages over all neutron paths of the line integral along the transmission direction of the square of the local fluctuations in the average induction. In reciprocal space this boils down to

$$\alpha_{ij} = \frac{8\pi^4}{Ly_0z_0}\int_{\tilde{K}} \Delta B_i(\mathbf{q})\Delta B_j(\mathbf{q})d^2\mathbf{q}, \qquad i,j = x,y,z, \tag{5}$$

where $\tilde{K}$ is the reciprocal yz plane and y_0 and z_0 are the dimensions of the neutron diaphragm in the corresponding directions.

The depolarization in a part with transmission length L will be denoted by the matrix

$$\underline{D}_L = \begin{pmatrix} 1-a(\alpha_{zz}+\alpha_{yy}) & a\alpha_{xy} & a\alpha_{xz} \\ a\alpha_{xy} & 1-a(\alpha_{zz}+\alpha_{xx}) & a\alpha_{yz} \\ a\alpha_{xz} & a\alpha_{yz} & 1-a(\alpha_{xx}+\alpha_{yy}) \end{pmatrix}, \tag{6}$$

where the constant a is defined by $a \equiv c^2\lambda^2 L$.

By combining Eqs. (4) and (6), a model matrix can be derived which simulates the change of the polarization vector of the beam while the neutrons are traveling through the whole sample. The derived matrix

$$\underline{D}_t = C^{-1}\int_{-3\Delta\lambda}^{3\Delta\lambda} e^{\left(\frac{\lambda-\lambda_0}{\Delta\lambda}\right)^2}\underline{Q}(\underline{R}\,\underline{D}_L\underline{R})^N\underline{P}d\lambda \tag{7}$$

describes an average of the theoretical model of the depolarization matrix over the wavelength distribution. This distribution is approximated by a Gaussian with a width $\Delta\lambda = 0.014$ nm and a central wavelength $\lambda_0 = 0.16 \pm 0.01$ nm which are determined from a calibration experiment with empty beam. The quantity C^{-1} is the normalization of the integral. $\underline{D}_t$ is the matrix that will be adapted to the measured matrix $\underline{D}_m$ by changing the parameters in Eqs. (4) and (6).

In order to solve this complicated nine-parameter, nine-equation problem, a least-squares method is used. In this procedure, the statistical errors are used to normalize the difference between calculated and measured matrix elements. In this case the least-squares function is defined by

$$F = \sum_{i,j=x,y,z}\frac{(D_{t,ij}-D_{m,ij})^2 I_s}{(1-D_{m,ij})(2-D_{m,ij})}. \tag{8}$$

Minimizing F gives the following set of parameters: $\langle B_x\rangle$, $\langle B_y\rangle$, $\langle B_z\rangle$, α_{xx} α_{yy}, α_{zz}, α_{xy}, α_{xz}, α_{yz}. The first three parameters represent the rotation (precession) of the polarization vector; the next six represent the depolarization (shortening of the polarization vector).

II. DEPOLARIZATION IN SINTERED SUPERCONDUCTORS

When a sintered high-T_c superconductor is placed in a magnetic field, two different situations can be distinguished: one where the grain size d is larger than the penetration depth λ_g in the grain and the other where d is smaller than λ_g. In the first case, the field can only penetrate into the weak Josephson links between the grains. According to Ref. 4, in this situation the effective penetration depth λ_{eff} can be written as $\lambda_{\text{eff}} = \sqrt{\lambda_g\lambda_j}$, with λ_j the Josephson penetration depth. In the second case, the ceramic superconductor can be approached as a conventional type-II superconductor.

For the sample that is used in the experiments, it is reasonable to assume that the second case is valid (see the next section). In this case, with the flux assumed to be aligned along the z direction, the Fourier transform of the magnetic field can be written as (see Ref. 4)

$$B(\mathbf{q}) = \frac{\phi_0\delta(q_z)}{(2\pi)^2}\sum_i \frac{e^{-i\mathbf{q}_\perp\cdot\mathbf{r}_i}}{1+\lambda_{\text{eff}}^2 q_\perp^2}, \tag{9}$$

where $\mathbf{r}_i$ points to one vortex position in the two-dimensional vortex lattice, λ_{eff} is the penetration depth, $\delta(q_z)$ is the Dirac δ function, and ϕ_0 is one flux quantum

defined as $\phi_0 = h/2e = 2.07 \times 10^{-15}$ Wb, with h Planck's constant and e the electron charge.

In this particular case only the z component of B is nonzero. Therefore it can be seen from Eq. (5) that only α_{zz} is relevant. In order to calculate α_{zz} one has to substitute Eq. (9) in Eq. (5) and subtract the contribution of $\langle B \rangle$ in the integral:

$$\alpha_{zz} = \frac{\phi_0^2}{4\pi L y_0} \sum_{i,j} \int \frac{e^{iq_y(y_i - y_j)}}{(1 + \lambda_{\text{eff}}^2 q_y^2)^2} dq_y - \frac{L}{2} \langle B \rangle^2. \quad (10)$$

To obtain this equation,

$$\int dq_z \delta(q_z) \delta(-q_z) = \frac{z_0}{2\pi} \quad (11)$$

is used. The sum in Eq. (10) can be split into a part where $i = j$ and into a part where $i \neq j$. The first part is equal to the total number of flux lines in the cross section of the sample perpendicular to the field direction, which equals $\langle B \rangle L y_0 / \phi_0$. In the case where the flux density is low (the distance between vortices is much larger than the penetration depth), the interactions between vortices are weak. Therefore it is allowed to assume that the flux is randomly but homogeneously distributed throughout the sample and that every y distance between vortices is equally probable. For this reason, in the second part where $i \neq j$, the sum over i and j may be written as separate integrals by substituting $\frac{\langle B \rangle^2 L^2}{\phi_0^2} \int dy_i \int dy_j$ for the sum. From this integral one obtains, for $i \neq j$, $2\pi \langle B \rangle^2 L^2 y_0 \delta(q_y)/\phi_0^2$. Substituting this result in Eq. (10) and integrating over q_y leads to the following expression for α_{zz}:

$$\alpha_{zz} = \frac{\langle B \rangle \phi_0}{16 \lambda_{\text{eff}}}. \quad (12)$$

A similar derivation can be made for the case that the beam direction is along the direction of the magnetic induction. In this case, only α_{xx} contributes and it is not necessary to split the sample in small parts. The expression that is obtained in this situation is given by[4]

$$\alpha_{xx} = \frac{\langle B \rangle t \phi_0}{8\pi \lambda_{\text{eff}}^2}. \quad (13)$$

If all the N small sample parts are put together, one obtains for the total depolarization matrix $\underline{D}_t = (\underline{D}_L)^N$. If N is large enough and $\underline{D}_L$ is diagonal as in the above case, one may replace the off-diagonal elements by 0 and in the diagonal elements one may replace L by t [see Eq. (6)].

III. EXPERIMENT

The experiments are performed on a sintered $YBa_2Cu_3O_x$ sample of size $5.35 \times 20.55 \times 11.0$ mm^3 produced at the University of Twente by D. H. A. Blank by a citrate synthesis method.[13] Samples prepared by this method have a grain size between 1 and 10 μm, which can form clusters up to 100 μm. In Fig. 1 the experimental conditions of the sample are shown. Around the sample, a coil is wound which enables one to apply a field in the z direction. This direction is defined to be along the longest side of the sample. The sample is clamped in a magnetic short circuit to prevent flux, emerging from the sample, to affect the polarization of the beam outside the sample. The short circuit also simulates infinitely long flux lines because demagnetization fields are prevented. On the holder supporting the sample and short circuit, a heating wire is wound and a Ge resistor is mounted as a temperature sensor.

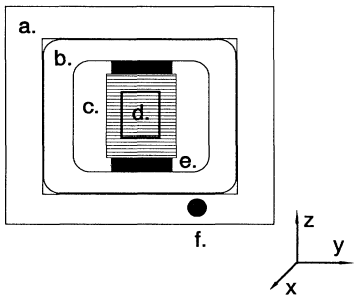

FIG. 1. Experimental setup of the sintered $YBa_2Cu_3O_{7-\delta}$ sample in the liquid-He cryostat. In the experiment x is the beam direction. Explanation of the letters in the picture: (a), holder and heater; (b), magnetic short circuit; (c), copper coil; (d), neutron diaphragm; (e), sample; (f), Ge temperature-dependent resistor.

After cooling the sample in zero field, a magnetic field has to be brought into the sample. This is done with the copper coil that is wound around the sample. Because of heating by the coil, the upper field limit at 4.2 K is about 0.05 T. In order to apply fields of considerable magnitude, the field is pulsed. The pulse that is used had a width of 500 μs and a peak value of 0.7 T. This field pulsing, however, presents another problem, namely, the high dB/dt, which is about 0.7 kT/s. This quick field input could be faster than certain relaxation times, leading to special flux distributions being captured.

IV. RESULTS AND DISCUSSION

With the values of λ_{eff} in the literature, it is possible to make an estimate of the depolarization by the vortices. In Ref. 14, λ_{eff} is given as measured in different experiments; at 4.2 K, $\lambda_{\text{eff}} \approx 200$ nm.

The results show that the remanent induction $\langle B \rangle \approx 0.01$ T at 4.2 K. In the setup described before, the transmission length $l = 5.36$ mm. Substituting these values in Eqs. (6) and (12) leads, with the magnetization perpendicular to the beam direction, to a depolarization $(\equiv 1 - \frac{|\mathbf{p}_f|}{|\mathbf{p}_0|})$ of 0.018%.

For the case where the beam direction is parallel to the magnetization, it follows from Eq. (13) that $\alpha_{xx} \sim t \lambda_{\text{eff}}^{-2}$. This dependence of the average line integral of the field fluctuation on the penetration depth does lead to a considerable depolarization, but a couple of practical prob-

lems such as beam divergence and alignment of the beam with the flux lines are not included in the calculation. Therefore the result in Eq. (13) represents an ideal situation that will be difficult to realize.

With the described instrument, the minimum depolarization that can be measured is about 0.5%, and so in the perpendicular field experiment no measurable depolarization by the vortices themselves is expected.

In Fig. 2, the depolarization matrix, as it is measured, is shown as a function of temperature. The calculated matrix is also drawn as a line through the points. It can be seen that the theoretical model describes the measured matrix very well.

The magnetization components fitted with the model are plotted against temperature in Fig. 3. This magnetization shows no measurable time dependence within 24 h, which is not consistent with magnetization measurements on the same sample. However, these magnetization measurements show a higher initial remanence and a relaxation to an almost stationary level which is larger than the remanence in our measurements. Furthermore, other ND experiments on a similar sample also show an absence of time relaxation.[5]

At low temperatures the remanent field decays faster than linear, probably caused by the fact that it is concentrated at the edge. Also, in the depolarization parameters, it appears that the flux lines are concentrated locally (as will be shown later). Above 40 K the decay is linear for reasons that will be explained later.

At low temperatures, besides a field in the applied direction, also field components appear in the perpendicular direction. These field components show that the flux lines are no longer straight, but are curved or meandering in bundles through the sample. Evidence that the flux is no longer straight also appears in the other calculated parameters.

In Fig. 4, $\alpha_{\parallel} \equiv \alpha_{zz}$ and $\alpha_{\perp} \equiv \alpha_{xx} + \alpha_{yy}$ are plotted against temperature (the nondiagonal elements of $\underline{D}_L$ are

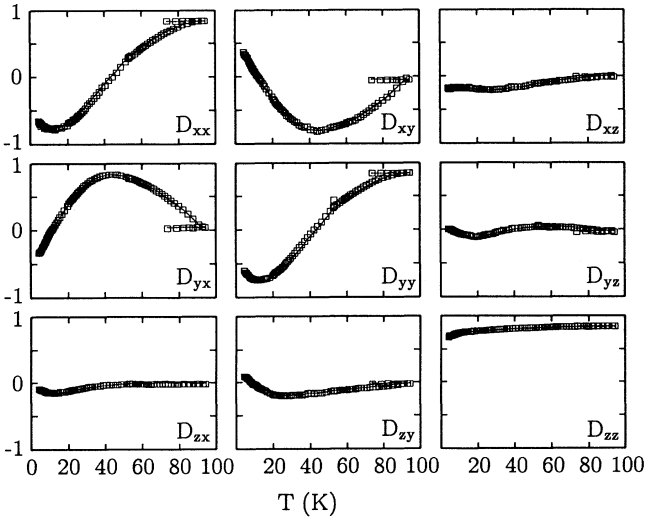

FIG. 2. Measured matrix (squares) and the theoretically calculated fit (drawn line) as a function of temperature.

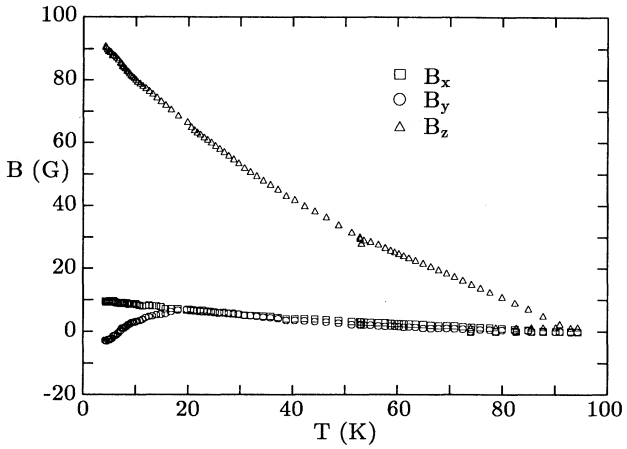

FIG. 3. Remanent magnetic field as a function of temperature, after zero-field cooling and a field pulse at 4.2 K.

0 within the statistical errors). Because of the large precession angle around the z axis, it is no longer possible to distinguish the fluctuations of the induction in the x direction from those in the y direction; therefore, the contribution of both directions is summed. By taking a look at the temperature dependence of $\alpha_{\perp}$ in Fig. 4(a), one can see that at low temperatures there is a contribution larger than zero. Because $\alpha_{\perp}$ can only contribute if there are local fluctuations perpendicular to the applied field, one must conclude that the trapped flux lines are bent. Furthermore, this bending must take place in bundles for arguments discussed before. One can think of such a bundle of flux lines bending around one pinning center when they try to move into the sample in the applied pulse. After the pulse they are captured in this bent situation. With the assumption that the perpendicular fluctuation of the remanent field is in the order of the average magnetization and with the knowledge that $\alpha_{\perp}$ is equivalent to the average of the square of the field fluctuation times a characteristic length, one can calculate an

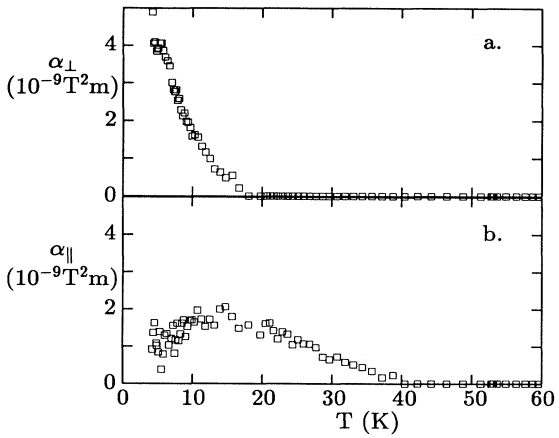

FIG. 4. Average of the squared field fluctuations perpendicular (a) and parallel (b) to the applied field, plotted as a function of temperature.

order of magnitude for the characteristic length. At 4.2 K this length is roughly 60 μm, decreasing rapidly to zero at 20 K. This length is of the same order of magnitude as the clusters that can be formed during preparation of the sample, but is one order of magnitude larger than the grain size. Between the clusters it is possible that some small holes exist, which are pinning the flux in bundles.

As argued before, the fact that at low temperatures $\alpha_{\|} > 0$, which corresponds to a depolarization according to Eq. (6), cannot be accounted for by the vortices themselves. Hence, it can be concluded that the flux is not homogeneously distributed.

When the temperature is raised after the field input, two processes take place. The first is thermal excitation; heating the sample "pushes" the vortices out of the pinning centers, allowing them more freedom to move. The second process is expansion of the vortices with increasing temperature. This expansion is caused by the fact that the closer the temperature is to T_c, the longer the penetration depth becomes. Because the penetration depth is directly related to the diameter of the vortices, the intervortex repulsion will act over a wider range around the vortex core.

As soon as the field pulse ends, the vortices are captured in their present position and shape, leading to a distribution of bent flux lines that is not homogeneous. When the temperature is raised, the vortices are excited out of the pin potentials and try to stretch to lower their volume and hence their field energy. At a temperature of 20 K, the pinning forces are no longer strong enough to keep the vortices bent, and so they all align. This alignment is seen in Fig. 4(a) as $\alpha_{\perp}$ going to zero. This means that field fluctuations are no longer present in the direction perpendicular to the applied field.

In the next temperature range between 20 K and 40 K, $\alpha_{\|}$ decreases linearly to zero [Fig. 4(b)]. This is caused by the intervortex repulsion. As stated before, the vortices obtain more freedom of movement with increasing temperature. This freedom allows them to choose a position with as little repulsion by neighboring vortices as possible, leading to a more homogeneous distribution of flux in the sample.

Above 40 K some remanent field is still present (Fig. 3), but no depolarization or field fluctuation is measured (Fig. 4). This means that there is a homogeneously distributed flux lattice present in the sample. The linear decay of the remanent field is caused by the expansion of the flux lines and lattice, resulting in a lower flux density. At the transition temperature T_c the remanent field disappears. This linear dependence of $\langle B \rangle = n\phi_0$, with n the density of vortices, leads to the conclusion that $\langle B \rangle \sim (1 - T/T_c)$. The lattice spacing is equal to 1 over the square root of the density. So the lattice spacing b is related to temperature in the following way:

$$b \sim \left(1 - \frac{T}{T_c}\right)^{-\frac{1}{2}} . \tag{14}$$

In a similar experiment to that described above but with a constant field of 2 kG applied for 2 h after zero-field cooling, the results were quite different. Because a superconducting coil was used in this experiment, no data could be obtained below the T_c=9.2 K of the coil wire, for reasons of depolarization by a remanent field in the coil. The temperature dependence of the remanent field after switching off the applied field is linear over the whole range from 9.2 K up to 100 K. Also over this range, no measurable depolarization is observed. From the latter remark it must be concluded that the field is homogeneously distributed. Again this indicates that the lattice spacing depends on the temperature as given in Eq. (14). Apparently with a pulsed field applied, the field inside the superconductor has no time to relax and is therefore captured in a chaotic situation. In the dc experiment the flux can relax while the field is still on, resulting in a homogeneous distribution being captured after the applied field is switched off.

V. CONCLUSIONS

In the described neutron-depolarization experiment on the flux distribution in sintered $YBa_2Cu_3O_x$, some remarkable effects are observed. From constant-field and pulsed-field experiments a clear influence of the method of field input can be seen on the distribution. After a pulsed-field input, the flux lines are bent in bundles and are not homogeneously distributed. After dc input of field a homogeneous distribution is observed. Both situations do not change in time.

With 3DND it is possible to measure the magnetization and the average local flux distribution throughout the sample as a function of the temperature at the same time. After pulsed input of field, the temperature dependence of the magnetization shows a nonlinear decay at low temperatures, changing to a linear dependence at 40 K where also the flux distribution becomes homogeneous. The fast decay at low temperatures is probably caused by a high flux density close to the sample edge.

In the temperature dependence of the distribution, three temperature areas can be observed. In the first area, between 4.2 K and 20 K, the flux is bent in bundles with a size of the same order of magnitude as the cluster size in the sample. With increasing temperature, the flux is stretching and is relaxed to a completely aligned distribution at 20 K. In the second area, between 20 K and 40 K, a relaxation to a homogeneous distribution is observed. At temperatures higher than 40 K, no depolarization is measured, leading to the conclusion that the distribution is homogenous up to T_c. The linear decay with temperature of remanent magnetization above 40 K leads to a temperature dependence of the lattice spacing according to Eq. (14).

ACKNOWLEDGMENTS

The authors would like to acknowledge D. H. A. Blank of the University of Twente for preparing the sample, used in the neutron depolarization experiments. We also would like to thank J. J. M. Franse, A. Gerber, and V. Duin of the University of Amsterdam for their helpful discussions and the magnetization measurements and B. P. Toperverg for his theoretical support.

[1] M. Yethiraj, H.A. Mook, G.D. Wignall, R. Cubitt, E.M. Forgan, D.M. Paul, and T. Armstrong, Phys. Rev. Lett. **70**, 857 (1993).
[2] H.W. Weber, J. Low Temp. Phys. **17**, 49 (1974).
[3] D. Petitgrand, B. Dillon, I. Mirebeau, G. Parette, and G. Collin, in *Proceedings of the ICTPS '90 International Conference on Transport Properties of Superconductors, Rio de Janeiro, Brazil, 1990* (World Scientific, Singapore, 1990), p. 175.
[4] L.A. Akselrod, G.P. Gordeyev, V.N. Zabenkin, I.M. Lazebnik, V.I. Sbitnev, and B.P. Toperverg, Physica B **174**, 354 (1991).
[5] R.J. Papoular and G. Collin, Phys. Rev. **38**, 768 (1988).
[6] M.L. Crow, R.J. Goyette, A.C. Nunes, S.J. Pickart, T.R. McGuire, S. Shinde, and T.M. Shaw, J. Appl. Phys. **67**, 4542 (1990).
[7] M.Th. Rekveldt, Z. Phys. **259**, 391 (1973).
[8] M.Th. Rekveldt, Text. Microstruct. **11**, 127 (1989).
[9] R. Rosman and M.Th. Rekveldt, J. Magn. Magn. Mater. **95**, 319 (1991).
[10] F.J. van Schaik, J.W. Burgmeyer, and M.Th. Rekveldt, J. Appl. Phys. **52**, 352 (1981).
[11] F.J. van Schaik, M.Th. Rekveldt, and J.W. van Dijk, J. Appl. Phys. **52**, 360 (1981).
[12] W. Roest and M.Th. Rekveldt, Nucl. Instrum. Methods A **322**, 65 (1992).
[13] D.H.A. Blank, H. Kruidhof, and J. Flokstra, J. Phys. D **21**, 226 (1988).
[14] B. Pümpin, H. Keller, W. Kündig, W. Odermatt, I.M. Savić, J.W. Schneider, H. Simmler, P. Zimmermann, E. Kaldis, S. Rusiecki, Y. Maeno, and C. Rossel, Phys. Rev. B **42**, 8019 (1990).